PCCP

Accepted Manuscript

This is an *Accepted Manuscript*, which has been through the Royal Society of Chemistry peer review process and has been accepted for publication.

Accepted Manuscripts are published online shortly after acceptance, before technical editing, formatting and proof reading. Using this free service, authors can make their results available to the community, in citable form, before we publish the edited article. We will replace this *Accepted Manuscript* with the edited and formatted *Advance Article* as soon as it is available.

You can find more information about *Accepted Manuscripts* in the Information for Authors.

ROYAL SOCIETY OF CHEMISTRY

www.rsc.org/pccp

De-agglomeration of multi-walled carbon nanotubes via the use of a novel organic modifier: structure and mechanism

Joyita Banerjee[1], Ajay S. Panwar[1], Kingsuk Mukhopadhyay[2], A. K. Saxena[2], Arup R. Bhattacharyya[1]*

[1]Department of Metallurgical Engineering and Materials Science

Indian Institute of Technology Bombay, Powai, Mumbai 400076, India

[2]Defence Materials and Stores Research and Development Establishment, Kanpur 208013, India

Abstract

The present investigation has dealt with the investigation of 'agglomeration' behaviour of two types of multi-walled carbon nanotubes (MWNTs; N-MWNTs and D-MWNTs), which primarily vary in the extent of chemical functionalities, average diameter and the extent of 'agglomeration'. The variation in the properties has been influenced by the varying 'agglomerated' structure associated with the respective MWNTs. The 'agglomerates' strength of the corresponding MWNTs 'agglomerates' has been estimated via nano-indentation experiment. It has been observed that the work done to indent D-MWNTs 'agglomerates' (3910.3×10^{-8} erg) was higher as compared to indent N-MWNTs 'agglomerates' (2316.4×10^{-8} erg). In this context, a novel organic modifier; Li salt of 6-aminohexanoic acid (Li-AHA) has been introduced to facilitate the 'de-agglomeration' of the MWNTs in the aqueous medium. The stability of the aqueous dispersion of Li-AHA modified MWNTs has further been analyzed using UV-visible spectroscopic analysis and zeta potential measurement. An increase in Li-AHA concentration has facilitated the dispersion state of MWNTs in the aqueous medium. Furthermore, the mechanism of dispersion of the two types of MWNTs in the aqueous medium in the presence of Li-AHA has been proposed based on the electrostatic charge repulsion between the negatively charged

species. Moreover, fluorescence activated cell sorting technique has been used to assess the extent of debundling of MWNTs 'agglomerates' in the aqueous medium. An attempt has been made to correlate morphology-property relationship studies in Li-AHA modified MWNTs.

*Author to whom all the correspondence should be addressed:

Prof. Arup R. Bhattacharyya

Contact number: Tel. No.: +91-22-2576-7634, Fax: +91-22-2572 6975

*Email ID: arupranjan@iitb.ac.in

Keywords: MWNTs, DC electrical conductivity, organic modifier, nano-indentation, fluorescence activated cell sorting.

Introduction

Carbon nanotubes (CNTs) are considered as one of the most promising materials with extraordinary structural and transport properties among the nano-filler category in the field of nanotechnology. CNTs could be utilized in a wide range of applications starting from field emission devices [1], biosensors [2], multi-functional composites [3], electrodes and actuators [4]. CNTs exhibit predominantly hydrophobic in nature. Due to the existence of high van der Waals force and high L/D ratio; CNTs exhibit a strong tendency to form 'agglomerates'. It has been reported that the performance of polymer/CNTs composites depends primarily on the effective dispersion of CNTs in the polymer matrices [5,6,7,8]. Further, uniform dispersion of CNTs in polymer matrix may lead to an effective stress transfer provided an adequate interfacial interaction exists between CNTs and the corresponding polymer phase, thus reinforcing the polymer matrix [9]. On the other hand, the pre-requisite to achieve electrically conductive polymer composites utilizing CNTs of low electrical percolation threshold would involve dis-entanglement of CNTs 'agglomerates' and subsequent dispersion of the smaller remaining 'agglomerates' or individualized CNTs within the polymer matrix [10,11,12]. In order to disperse CNTs 'agglomerates' uniformly in the aqueous medium, ultra-sonication [13] plays an important role, which involves the utilization of mechanical energy that leads to high local stress. The dynamics of the dispersion process was investigated by Vigolo et al. [14] using UV-visible spectroscopic analysis to optimize the ultra-sonication time to achieve the uniform dispersion of CNTs. CNTs treated with oxidizing acid exhibited improved dispersion of CNTs into fine fibrils [15]. In general, two methodologies viz. 'covalent' and 'non-covalent' approaches have been utilized to dis-entangle CNTs 'agglomerates'. Covalent methodology involves the attachment of organic moieties on sp^2 hybridized carbon atom of CNTs. However, the covalent

functionalization deteriorates the intrinsic electrical properties associated with CNTs. The approach of grafting PEG on the CNTs surface has also been studied, which shows stabilized CNTs dispersion [16]. Apart from these, researchers have shown interest on the functionalization via the use of long chain alkyl group viz., dodecyl group [17] on the CNTs surface. On the other hand, non-covalent methodology deals with non-disruptive interactions like π-π stacking, adsorption of surfactant on the surface of nanotubes [18] or columbic interaction of foreign moiety with the functional groups on nanotubes. In order to improve the dispersion state of CNTs in various solvents, dispersants or surfactants [19] have been added to overcome the intra-tube van der Waals force of attraction. During the process, various forces viz., electrostatic forces, hydrophobic interactions, π-π interactions, hydrogen bonding and even adsorption of organic molecules [20] could establish between the dispersant and the CNTs. Moreover, an optimal ratio for CNTs to modifier could lead to best dispersion state. Surfactant of lesser amount [21] may lead to incomplete coverage of surfactant on the CNTs surface and higher amount of surfactant may lead to segregation of surfactant molecules exhibiting poor dispersion (micelle formation) [22]. Moreover, the state of dispersion of the CNTs depends on the tail length of the hydrophobic part [23], functionality [24] and the polarity of the surfactant [25].

A majority of the research work has focused on dispersing CNTs in the aqueous medium utilizing two approaches, viz.; (a) by increasing the steric hindrance by the molecules adsorbed on the surface of the CNTs or (b) by exploiting the absolute zeta potential value of the modifier, which may induce the electrical double layer on the nanotubes 'agglomerates'. In this context it is to be noted that lithium salt of 6-aminohexanoic acid (Li-AHA) may act as an efficient dispersant in improving the dispersion state of MWNTs in PP/PA6 blend system [26] and in case of hybrid nano-filler based PA6 nanocomposites [27].

In view of this, an attempt has been made to investigate the 'de-agglomeration' behaviour of two different types of MWNTs (obtained from different sources) in the aqueous medium using a novel organic modifier, Li-AHA. In fact, the 'de-agglomeration' of MWNTs in the aqueous medium primarily depends on the 'agglomerates strength' of the MWNTs 'agglomerates'. In this context, the 'agglomerates strength' of the MWNTs has been estimated through nano-indentation technique. Nano-indentation technique has been used as an efficient tool to determine the micro-mechanical properties and has been used by several research groups [28-29] to determine the micro-mechanical properties of the nanofillers. Further, this technique has been used for the first time in the present context to determine the micro-mechanical properties associated with MWNTs 'agglomerates'. Moreover, fluorescence activated cell sorting (FACS) technique is an extremely outstanding technique to determine the size and the granularity of the particles. FACS technique could be used to analyze the cell particles and has been primarily restricted in the biomedical field [30-31]. In the present context, this technique has been utilized to assess the role of Li-AHA in dispersing MWNTs 'agglomerates' in the aqueous medium. Furthermore, an extensive investigation has been carried out to address the influence of Li-AHA on the MWNTs 'agglomerates' strength. Mechanism of the 'de-agglomeration' of MWNTs in the presence of Li-AHA has also been postulated.

Experimental

Materials and modifications

Purified multi-walled carbon nanotubes (MWNTs) were procured from Nanocyl S.A., Belgium (NC 3100). The average length and average diameter of the MWNTs (hereafter will be referred as N-MWNTs) are ~ 1.5 µm and ~ 9.5 nm respectively. The second category of

MWNTs (D-MWNTs) was synthesized in DMSRDE, Kanpur, which exhibit an average diameter of ~ 13 nm and the purity of < 90%. MWNTs were further modified with an organic modifier (lithium salt of 6-amino hexanoic acid) as follows:

6-aminohexanoic acid (AHA from Sigma Aldrich, Germany) was neutralized by lithium hydroxide in de-ionized water to obtain the lithium salt of 6-aminohexanoic acid (Li-AHA). MWNTs were ultra-sonicated in de-ionized water for 20 min. In order to reach the pre-determined weight ratio of a:b; wherein a = MWNTs and b = Li-AHA; a requisite amount of Li-AHA was added to MWNTs dispersion and were further ultra-sonicated in de-ionized water for 10 min. Li-AHA modified MWNTs dispersion was then allowed to undergo evaporation at 100 °C. Further, the mixture was dried at 80 °C under vacuum oven for 24 h to ensure the complete removal of water from the dried powder. Table 1 depicts the compositions and the corresponding nomenclature used in the work.

Table 1: Compositions and nomenclature used for various MWNTs

Trade name of MWNTs	Source	Abbreviation used for MWNTs	Abbreviation used for MWNTs modified with Li-AHA (x = 1, 4, 6 and 8)
NC3100	Nanocyl S.A., Belgium	N-MWNTs	N-MWNTs : Li-AHA (1: x) (wt/wt)
MWNTs obtained from India	DMSRDE, Kanpur, India	D-MWNTs	D-MWNTs : Li-AHA (1: x) (wt/wt)

Characterization techniques

Optical microscopic analysis was carried out using Olympus optical microscope (Gx51, USA). 3 mg of either pristine or Li-AHA modified MWNTs were dissolved in 50 ml of de-ionized water and were ultra-sonicated for a very short period of time in order to restore the

dispersion state of MWNTs in the aqueous medium. A drop of the dispersion was put on a glass slide and was covered with a covering slide in order to restore the distribution of MWNTs. Average diameter of the MWNTs 'agglomerates' was evaluated from Olysia m3 software using the corresponding optical micrographs. The %error in determining the average 'agglomerates' size of MWNTs was less than 5%.

Scanning electron microscopic (SEM) analysis was carried out for the pristine MWNTs with the help of field emission electron microscope JSM-7600F (Jeol, Japan) at an accelerating voltage of 10 kV. Pristine MWNTs were dispersed in de-ionized water and ultra-sonicated for 10 min, afterwards a drop of the corresponding dispersion was placed on a carbon paste coated stub.

Transmission electron microscopic (TEM) analysis was carried out with the help of field emission electron microscope JEM-2100F (Jeol, Japan). 3 mg of pristine MWNTs were dispersed in 20 ml of de-ionized water, whereas Li-AHA modified MWNTs were dispersed in 20 ml of iso-propyl alcohol and were sonicated for 10 min. Then, a drop of the dispersion was placed on the TEM grid and dried for a longer period of time in order to remove water completely.

Nano-indentation experiment was performed on compacted MWNTs pellets (diameter = 10 mm and thickness = 2 mm) with TI-900 (Hysitron Inc., Minneapolis, USA). MWNTs pellets were prepared by pressing MWNTs into a die using a hydraulic press at a pressure of 100 kN and also at 50 KN for 2 min. The constant indenting force used for detecting the MWNTs 'agglomerates' was kept 20 μN with loading/unloading time of 8 sec and holding time of 5 sec. A low load Berkovich indenter [32] was used as a tip.

Fluorescence activated cell sorting (FACS) experiment was carried out in BD FACS Aria II Special Order System, which was equipped with FSC/SSC detector with a 488 nm laser.

Raman spectroscopic analysis was carried out for the pristine and Li-AHA modified MWNTs with HR 800 micro-Raman (HORIBA, Jobin Yovon Technology, and France). An incident laser with excitation wavelength of 514 nm was utilized in the scanning range of 200 to 2000 cm^{-1}.

XPS analysis was carried out using the MULTILAB (Thermo VG Scientific, USA), equipped with concentric hemispherical analyser. O 1s and C 1s scans were carried out in order to identify the elemental compositions and the functional groups present on the surface of MWNTs. The X-ray used was Al K$_\alpha$ with the take-off angle of 90°, with the resolution of 0.5 eV for the HR scan. The energy for the survey scan was 100 eV with the resolution of 2 eV.

Brunauer-Emmet and Teller analysis (BET) was carried out to estimate the specific surface area of pristine and Li-AHA modified MWNTs. Specific surface area measurements were carried out using surface area analyzer (Smart Instruments, Thane, India) with the aid of nitrogen adsorption technique.

Zeta potential measurements were carried out using Beckman Coulter Delsa Nano C. 3 mg of MWNTs were ultra-sonicated in 75 ml de-ionized water for 15 min. Zeta potential values were measured at five points across the capillary and were repeated for five times.

 UV-vis spectroscopic measurements were carried out using UV Jasco V650 dual beam spectrophotometer (Jasco Analytical Instruments, Japan). 3 mg of MWNTs were ultra-sonicated in 75 ml de-ionized water for 10 min.

The pH measurements were carried out using pH-meter (PCi Analytics, India) standardized with pH 4.01 and 7.01 buffer solutions.

DC electrical conductivity of the compacted MWNTs pellets of pristine and Li-AHA modified MWNTs was measured using Novocontrol Technologies (Alpha A analyzer; 3 μHz -

20 MHz) with Agilent E4991A RF analyzer (1 MHz - 3 GHz, Germany) in the frequency range between 10^{-1} to 10^6 Hz. DC electrical conductivity was obtained from the low frequency plateau of the AC electrical conductivity versus frequency plot by fitting Jonscher's 'Universal Power law' equation ($\sigma_{AC} = \sigma_{DC} + A\omega^n$, $0<n<1$), where 'A' is the constant dependent on temperature and 'n' is an exponent dependent on the frequency as well as on the temperature.

Results and Discussion

a. Characterization of MWNTs

Figure 1 shows the various parameters associated with N-MWNTs and D-MWNTs. It is observed that the average 'agglomerates' size of N-MWNTs is 66.5 μm, whereas D-MWNTs exhibit an average 'agglomerates' size of 135.4 μm. SEM analysis suggests a dense entangled structure associated with N-MWNTs, whereas 'agglomerated' structure along with dense entangled network are observed corresponding to D-MWNTs. N-MWNTs show an average diameter of 10.2 nm, which is marginally lower than D-MWNTs (13.6 nm). Higher entangled network is observed also in case of D-MWNTs from the TEM analysis. In brief, microscopic analysis suggests higher average 'agglomerates' size corresponding to D-MWNTs (with a higher entangled network) as compared to N-MWNTs. The 'aggregate' size obtained from DLS studies could also confirm a similar trend. Moreover, BET analysis shows a higher specific surface area corresponding to N-MWNTs (280 m^2/g) as compared to D-MWNTs (207 m^2/g), which indicates 'agglomerates' structure with higher porosity corresponding to N-MWNTs. A similar observation [33] has been reported earlier, which shows a specific surface area of N-MWNTs of ~ 269.9 m^2/g corresponding to N-MWNTs.

X-ray photoelectron spectroscopic analysis suggests a higher fraction of oxygen functionality associated with D-MWNTs as compared to N-MWNTs. This observation can be substantiated by the observed pH values corresponding to the respective aqueous dispersion of N-MWNTs and D-MWNTs.

Raman spectroscopic analysis indicates a higher I_D/I_G ratio corresponding to D-MWNTs as compared to N-MWNTs, which suggests a higher fraction of ordered graphitic structure, is associated with N-MWNTs. N-MWNTs exhibit I_D/I_G ratio of 0.95. However, the reported value from earlier work [25] suggests I_D/I_G ratio of 1.18 corresponding to N-MWNTs, which may be attributed to the batch to batch variation during the production of N-MWNTs. Further, I_D/I_G ratio also indicates a higher fraction of defects/ disordered structure associated with D-MWNTs. Raman spectra (not shown here) of the MWNTs exhibit the characteristic peaks for MWNTs, which are observed at 1347 cm^{-1} and 1590 cm^{-1} in the tangential mode. A peak associated with the D-band was observed around ~1330 cm^{-1}, which corresponds to the defects present in the graphitic structure. A peak occurring in the range of 1550–1600 cm^{-1} range constitutes the G-band [19]. In graphite, a single peak is present at 1582 cm^{-1} and corresponds to the tangential vibrations of the carbon atoms. Further, a peak has been observed (not shown here) at 2700 cm^{-1}. This peak has been considered as a overtone or second order mode of D-band and is termed as 2D band [34]. This occurs due to two phonon second order scattering process.
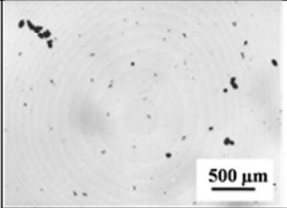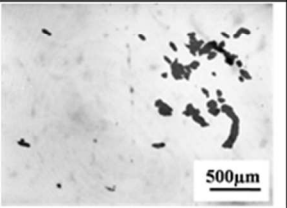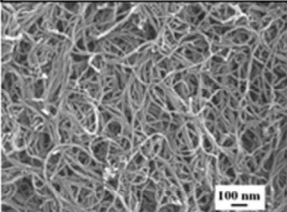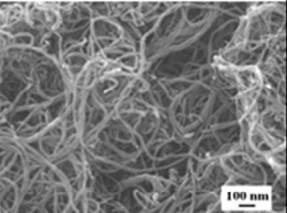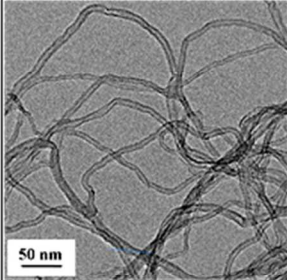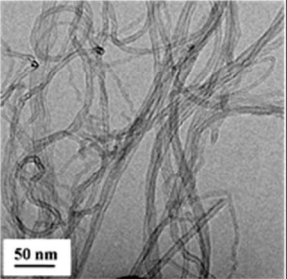
Characterization techniques	Information obtained	N-MWNTs	D-MWNTs
Optical microscopic Analysis	Average 'Agglomerates' size (μm)		
		66.5	135.4
SEM Analysis	State of Entanglement		
TEM Analysis	Average Diameter (nm)		
		10.2	13.6
BET	Specific surface area (m^2/g)	280.3	207.4
X-Ray Photoelectron Spectroscopic Analysis	Graphitic Carbon Content (%)	80	75.2
	Carbon Content (atomic %)	92.2	91.3
	Oxygen Content (atomic %)	7.7	8.7
Raman Spectroscopic Analysis	I_D/I_G	0.95	1.09
	I_G/I_{2D}	0.56	1.1
pH	pH- values	6.8	5.7
DLS	Aggregate size (nm)	414.6	476.3

Figure1: Characterization of various types of MWNTs (N-MWNTs and D-MWNTs)

Dileo et al. [35] mentioned that the parameter I_D/I_G could not be considered as a straightforward way due to the effect of carbon impurities and thus, the parameter I_{2D}/I_G could be considered as an accurate alternative to estimate ordered/disordered ratio corresponding to a specific MWNTs. Further, Gupta et al. [36] showed that the electronic properties of the graphene could be related to the shape of 2D band and I_G/I_{2D} ratio might provide an idea of the number of layers present in the graphene structure.

The intensity ratio of I_G/I_{2D} is related to the number of layers by the following equation:

$$\frac{I_G}{I_{2D}} = 0.14 + \frac{n}{10} \quad \text{.......} (1)$$

where, 'n' indicates the number of layers and I_G/I_{2D} value suggests the ratio of the intensity of G-band to that of the 2D band. From the equation 1, it is clear that the number of layers increases linearly with the increase in the intensity ratio of I_G/I_{2D}. Hence, higher value corresponding to I_G/I_{2D} ratio suggests higher number of layers involved in the MWNTs. It can also be observed (Figure 1) that N-MWNTs exhibit a lower value of I_G/I_{2D} ratio, which suggests lower number of walls present as compared to D-MWNTs.

b. Influence of the novel organic modifier; Li-AHA on the 'de-agglomeration' of MWNTs 'agglomerates'

It is reported that various secondary forces of attractions viz., surface and field forces, van der Waals, electrostatic forces and magnetic forces [37] could lead to 'agglomeration' in MWNTs. However, at the nanoscale level, van der Waals force [38] dominates over the gravitational force and thus, contributes maximum in developing MWNTs 'agglomerates'. This may also imply that in order to breakdown MWNTs 'agglomerates', cohesive force between the

MWNTs should be minimized. It has been reported that the magnitude of force existing in case of bundled SWNTs or entangled MWNTs network is observed to be 500 eV μm^{-2} [39,40] . It has also been reported that the van der Waals force of attraction (vdW) decreases with increase in outer diameter of the nanotubes [41]. In the present context, it is observed that the value of outer diameter increases with increase in Li-AHA content, which may definitely decrease the force of attraction between the nanotubes, thus facilitating the 'de-agglomeration' of MWNTs

MWNTs form a colloidal dispersion involving MWNTs 'agglomerates' as dispersed phase in an aqueous medium. The instability of the colloidal dispersion can be thermodynamically expressed as:

$$dw = \gamma dA \ \ldots\ldots\ (2)$$

where, γ is surface tension or surface energy of the solvent and is defined as the work done to alter the surface area of the liquid by unit area, dA is the change in surface area and dw is the work done. It is known that at constant temperature and constant pressure:

$$dw = dG \ldots\ldots\ (3)$$

Thermodynamically, dG< 0 denotes the spontaneity of the process that would be only possible when dA<0. Hence, in order to decrease the interfacial energy, the 'dispersed' phase (MWNTs) may form 'agglomerates' leading to colloidal coagulation and may even lead to phase separation. Moreover, the colloidal stability of MWNTs dispersion is primarily controlled by the sum total of the interparticle potential energy (V_T):

$$V_T = V_{vdw} + V_e + V_{Steric} + V_{Solution} \ \ \ \ \ldots\ldots\ (4)$$

where, V_T represents the total interparticle potential energy, V_{vdw} represents attractive long range van der Waals force existing between the particles, V_e denotes repulsive potential energy due to electrostatic interaction between the particles, V_{Steric} denotes repulsive adsorbed species and $V_{Solution}$ represents potential energy possess due to non-adsorbed ions. V_e is related to the surface charges of the particles.

In order to overcome the 'agglomerated' structure of MWNTs, a novel organic modifier (Li-AHA) has been utilized wherein, it is expected that Li-AHA may also act like a classical surfactant, which may induce electrostatic force of repulsion between the negatively charged species. This process may eventually lead to the dispersion of 'individualized' MWNTs in the aqueous medium, which on evaporation leads to porous MWNTs 'agglomerates', wherein Li-AHA would be adsorbed on the MWNTs surface. A higher content of Li-AHA may lead to higher fraction of 'individualized' MWNTs with 'agglomerates' structure of smaller size. In this context, it is to be noted that the 'agglomerates' strength of MWNTs plays an important role in the dispersion state of MWNTs in any medium (solvent or polymer matrix).

Nano-indentation is one of the characterization techniques by which the micro-mechanical properties of CNTs could be estimated. The basic principle of nano-indentation technique involves the approach of a well-defined tip into the surface of a specimen and then retrieval of the tip after indentation. This method was initially used to determine the mechanical properties, viz., hardness, elastic modulus of ceramic materials. Kendell and Weihs et al. [20] reported the elastic and plastic behavior of spray dried 'agglomerates' of zirconia particles under compression mode. It has been observed that before ultimate deformation, the 'agglomerates' exert certain amount of resistance followed by both elastic and plastic deformation. The micro-

mechanical behavior of the silica 'aggregates' was studied by Schilde et al. [42] by using nano-indentation technique, where it was mentioned that the Hertzian contact theory was followed at low indentation depth. Similarly, Raichman et al. [21] investigated the 'agglomerates' strength of silver nano-particles using nano-indentation technique and a different mechanism of deformation during indentation was observed. Figure 2 shows load versus displacement plot for the compacted MWNTs pellets corresponding to N-MWNTs and D-MWNTs. The shape of the curve may not only provide information about hardness and the modulus of the material, but also responsible to detect certain nonlinear events like cracking, phase transformation and even porosity. In case of indentation curve, the integration over the loading cycle may provide the total work including both elastic and plastic work, whereas integration over the unloading cycle may only provide the elastic work [43]. The area under the curve of load versus displacement plot during the loading cycle provides an idea about the energy dissipated during deformation of the MWNTs 'agglomerates'. Hence, the area under the loading curve may be considered as the work done to deform MWNTs 'agglomerates'. It is to be noted that for an ideal elastic material, there exists no difference between the loading and unloading cycle. The most well-known model that estimates the elastic modulus of the bulk material is 'Oliver and Pharr' method [44]. This model involves the fitting of the unloading portion of the load-displacement curve to the power law relation as provided below [45]:

$$F = B\,(h - h_f\,)^m \ \ldots\ldots\ldots\ (5)$$

where, 'B' and 'm' are the fitting parameters, 'h_f' is the final depth due to indentation after complete removal of indentation load.

The hardness and modulus of the specimen can be obtained from the slope of the unloading curve. The reduced modulus obtained from the contact between the rigid indenter of definite shape and homogeneous specimen is provided by:

$$E_r = \frac{1}{2\sqrt{\frac{\pi}{A(h_c)}}} \left(\frac{dp}{dh}\right) \quad \ldots\ldots\ldots (6)$$

where, E_r is the reduced modulus, dP/dh is the contact stiffness, $A(h_c)$ is the indentation area.
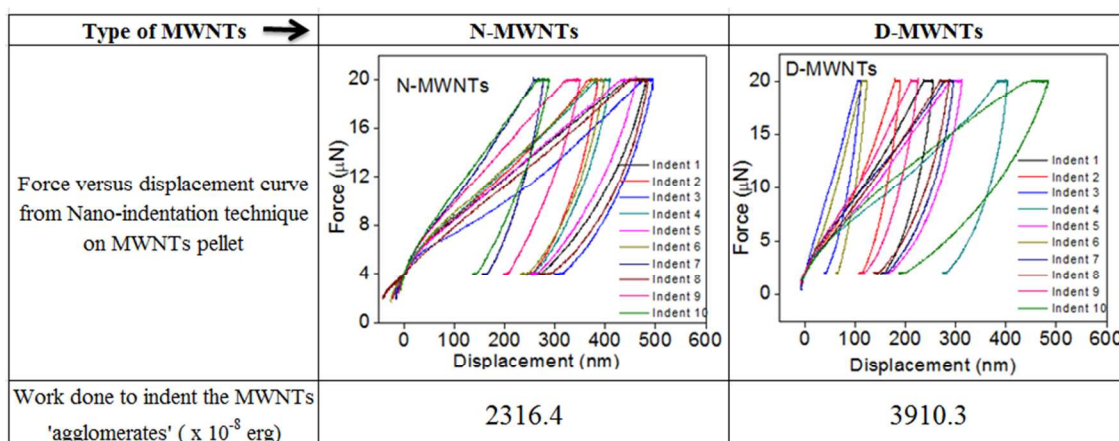

Type of MWNTs ➡	N-MWNTs	D-MWNTs
Force versus displacement curve from Nano-indentation technique on MWNTs pellet		
Work done to indent the MWNTs 'agglomerates' (x 10⁻⁸ erg)	2316.4	3910.3

Figure 2: Load versus displacement curves for compacted MWNTs pellets obtained from nano-indentation measurement

The equation (6) has been further modified by Sneddon and Brotzen, the Young's modulus of MWNTs can be obtained from the equation (7):

$$\frac{1}{E_r} = \frac{1 - \gamma_{particle}^2}{E_{particle}} + \frac{1 - \gamma_i^2}{E_i} \quad \ldots\ldots\ldots (7)$$

where, E_r is reduced modulus obtained from unloading curve of nano-indentation and E_i (1140 GPa) and γ_i (0.07) are the Young's modulus and Poisson's ratio of the low load Berkovich indentor.

16

Figure 2 exhibits that higher force is required to indent D-MWNTs pellets as compared to N-MWNTs pellets at a constant load. Thus, the indentation on MWNTs could be considered as an effective technique to estimate the 'agglomerates' strength of MWNTs, which otherwise would detect to compare the strength of various MWNTs 'agglomerates' at a given load value. The %error value corresponding to the nano-indentation experiment is considerably high, which may be attributed to the difference in the local micro-structural features present near the vicinity of the indented point. A similar observation was also observed by Gong et al. [46] for high purity fine grained alumina particles. The value of the displacement could be higher, when the indenter tip encounters with a softer entity as compared to other features. Hence, in order to get moderate average values corresponding to the nano-indentation experiment at least 25-30 points were chosen for indentation corresponding to each sample and an average value has been considered.
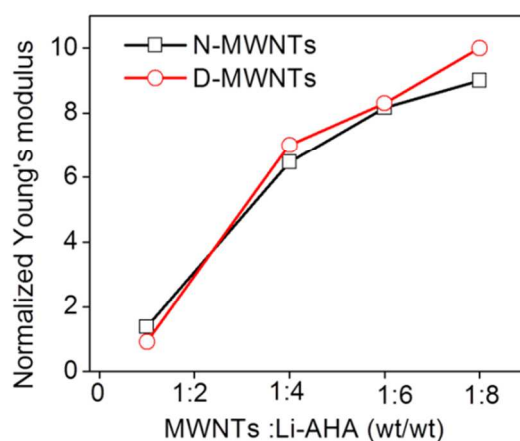
Figure 3: Variation of normalized Young's modulus as a function of Li-AHA concentration in the corresponding pellets of MWNTs/Li-AHA solid mixture

Figure 3 exhibits the variation of normalized Young's modulus corresponding to MWNTs pellets with increase in Li-AHA concentration in the corresponding pellets comprising of MWNTs/Li-AHA mixture. It is observed that with increase in Li-AHA content, the Young's

modulus of the pellet of MWNTs/Li-AHA mixture increases irrespective of the type of MWNTs. In this context, it is to be noted that the pellets consisting of pristine N-MWNTs and D-MWNTs exhibit Young's modulus of 1.2 GPa and 0.87 GPa respectively.

This observation can be explained on the basis that with increase in Li-AHA concentration, the 'de-agglomeration' of MWNTs is facilitated, which leads to smaller 'agglomerates' along with 'individualized' MWNTs. It is known that 'individualized' MWNTs exhibit higher modulus as compared to 'agglomerated' MWNTs. However, it is observed that the value of the work done to indent MWNTs 'agglomerates' decreases from 1418.7×10^{-8} erg for the pellet consisting of 1:1 N-MWNTs:Li-AHA mixture to 193.2×10^{-8} erg for 1:4 N-MWNTs:Li-AHA mixture, 96.2×10^{-8} erg for 1:6 N-MWNTs:Li-AHA mixture and 50.8×10^{-8} erg for 1:8 N-MWNTs:Li-AHA mixture. Moreover, the displacement value increases with wide variation of results, which suggests the formation of 'porous' structure due to the presence of Li-AHA.

FACS technique is a unique and an alternative technique to investigate the extent of dispersion of MWNTs in the aqueous medium in the presence of Li-AHA. FACS technique has been used to ascertain the size distribution of particles or cells with their size varying between 0.5 to 70 μm [47]. In this technique, the sample has been dispersed in a solvent medium and was injected into a column. In the column, it will take a laminar flow path forming a single file. A single wavelength laser has been used to illuminate each cell or particle producing an event.
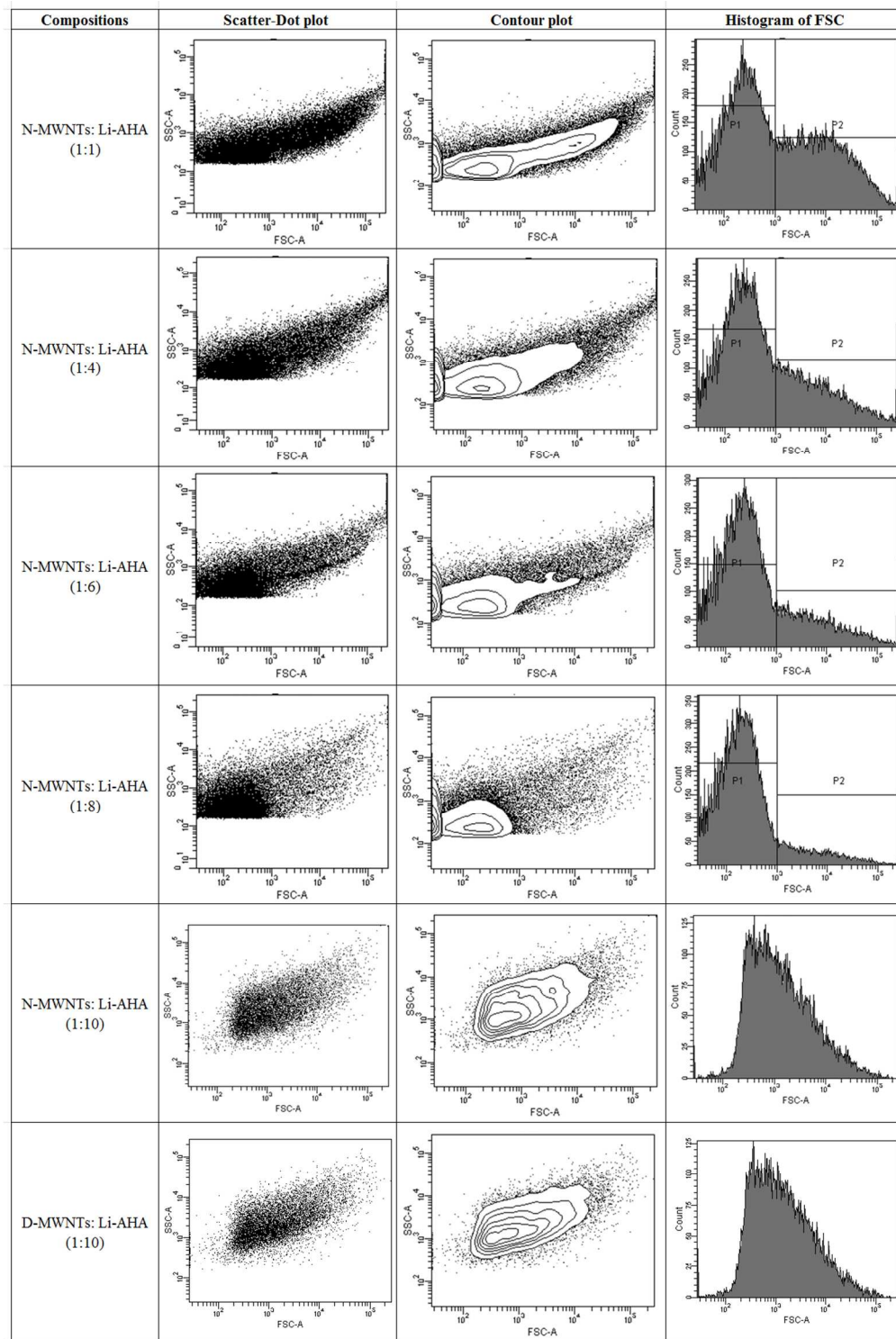
Figure 4: Scatter-dot plot, contour plot for Li-AHA modified N-MWNTs and D-MWNTs

obtained from FACS experiment

When the laser encounters with a particle or a cell, it generates forward scatter and side scatter, typically represented as forward scatter count (FSC) and side scatter count (SSC) respectively. The study involves bi-variate plot of SSC and FSC, which is related to the granularity and the surface area ('agglomerates' size) of the particles respectively. FACS involves simultaneous accumulation of information of size distribution of particles or cells along with statistics and valuable information for the structural complexities developed in the aqueous medium. FSC signal represents the cross-sectional area of the biological cells and thus, in this case it will act as a parameter to assess the particle size. However, SSC depends on the internal complexities of the cell, their roughness, shape and as well as their way to deflect the light. In the current context, the extent of dispersion of MWNTs has been indirectly studied through the size distribution of MWNTs obtained from bivariate FSC-SSC plot.

Figure 4 represents the scatter-dot plot for the Li-AHA modified MWNTs along with the histogram showing the distribution of various sizes of MWNTs 'agglomerates'. Figure 4 also shows the 'scatter-dot' plot for different types of MWNTs dispersed in de-ionized water with the aid of Li-AHA. However, it was difficult to attain a stable dispersion of D-MWNTs in the de-ionized aqueous medium at low Li-AHA concentration. Hence, D-MWNTs were dispersed in the de-ionized water in the presence of Li-AHA in the ratio of 1:10 (wt/wt). In general, MWNTs exhibit high aspect ratio, and form 'agglomerates' structure, which leads to the appearance of MWNTs population along the diagonal of the FSC-SSC plot. It was observed earlier that as the size of MWNTs 'agglomerates' decreases, MWNTs population was shifted to lower scatter value, but still the population of MWNTs would maintain a diagonal relationship between FSC and SSC. Moreover, the plots clearly show two populations of size distribution corresponding to MWNTs 'agglomerates' viz., P1 and P2. Tiwari et al. [48] also reported earlier regarding the two

types of populations, wherein P2 corresponds to tubular structure associated with MWNTs and P1 corresponds to particulate characteristics. In the current context, N-MWNTs and D-MWNTs depict two populations – P1 and P2 at various weight ratios of MWNTs: Li-AHA viz., 1:1, 1:4, 1:6 and 1:8 (wt/wt), whereas for the weight ratio of 1:10 (wt/wt) MWNTs/Li-AHA, plot shows one population. The contour plot represents the density of the group of the particles for a specific population. It is observed that the population P2 decreases with increase in weight fraction of Li-AHA, which suggests the breakdown of MWNTs 'agglomerates' in the presence of Li-AHA.

Figure 5 depicts that the value of FSC-A for N-MWNTs is lower as compared to D-MWNTs, which suggests the existence of smaller 'agglomerates' in case of N-MWNTs as compared to D-MWNTs at higher concentration of Li-AHA. It can also be observed (Figure 5a) that with increase in the modifier content, the value of SSC-median increases. In fact, SSC-median represents the granularity of the particles. Cai et al. [30] reported SSC as a parameter to study the interaction between the mammalian cells and CNTs. It was mentioned that the amplitude of SSC was proportional to the amount of CNTs associated with the cells. In the current context, it has been observed that the value of SSC-median is increased with increase in Li-AHA content, which indicates further the breakdown of MWNTs 'agglomerates' into smaller entities in the presence of Li-AHA via the electrostatic charge repulsion between Li-AHA and MWNTs [19].

A similar observation was also reported by Haniu et al. [31], where the effect of various dispersants on the state of dispersion of VGCF has been studied through flow cytometry. It was observed that the value of SSC was increased with the addition of the dispersant to VGCF.
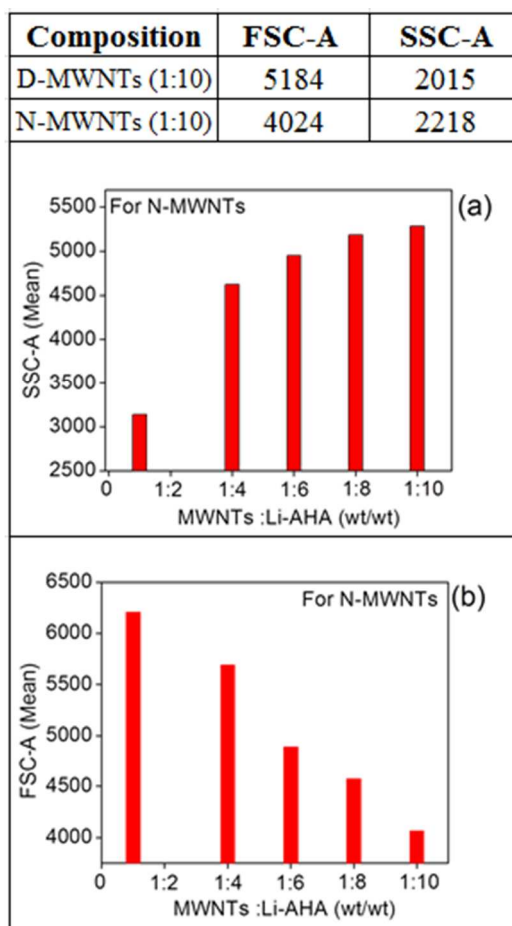
Composition	FSC-A	SSC-A
D-MWNTs (1:10)	5184	2015
N-MWNTs (1:10)	4024	2218

Figure 5: Variation of FSC-A (median) and SSC-A values as a function of Li-AHA

concentration in Li-AHA modified MWNTs

c. The mechanism of 'deagglomeration' of various MWNTs by the non-covalent modifier; (Li–AHA)

TEM micrographs of the MWNTs modified with varying proportions of organic modifier (Li-AHA) are shown in Figure 6. It is observed that with addition of Li-AHA, the extent of entanglement within the nanotubes 'agglomerates' is decreased, which confirms the fact that Li-AHA facilitates 'deagglomeration' of the MWNTs in the aqueous medium. Moreover, the dis-entanglement of the MWNTs 'agglomerates' is more prominent with increase in Li-AHA

content, which suggests the role of Li-AHA in effective 'debundling' of MWNTs. It is further observed that the average diameter of both the types of MWNTs increases with Li-AHA concentration in Li-AHA modified MWNTs. Addition of Li-AHA to N-MWNTs leads to an increase in the average diameter of N-MWNTs from 10.2 nm (for pristine N-MWNTs) to 11.6 nm for 1:1 N-MWNTs:Li-AHA (wt/wt) and 14.6 nm corresponding to 1:8 N-MWNTs:Li-AHA (wt/wt). In a similar way, for D-MWNTs, the average diameter increases from 13.6 nm (for pristine D-MWNTs) to 14.1 nm for 1:1 D-MWNTs:Li-AHA (wt/wt) and 15.8 nm for 1:8 D-MWNTs:Li-AHA (wt/wt). A similar observation [26] has been reported earlier for N-MWNTs, which shows an increase in the average diameter of N-MWNTs (from ~ 9.04 nm to ~ 9.59 nm) due to the presence of adsorbed Li-AHA onto MWNTs surface. Average 'agglomerates' size of MWNTs obtained from optical microscopic analysis (Figure 6) shows a progressive decrease as a function of Li-AHA concentration. A similar observation has also been reported for MWNTs modified with Na-AHA and PyCHO, which showed a decrease in 'agglomerates' size of MWNTs from 73.3 μm to 59.9 μm for Na-AHA and to 24.3 μm for PyCHO modified MWNTs [49]. However, the 'agglomerates' size of Li-AHA modified D-MWNTs is higher as compared to the 'agglomerates' size of Li-AHA modified N-MWNTs irrespective of any composition. This observation suggests the role of Li-AHA in breakdown of MWNTs 'agglomerates', however, the extent of de-agglomeration depends on the respective 'agglomerates' strength of N-MWNTs and D-MWNTs.

Table 2 elaborates various parameters in connection with Li-AHA modified MWNTs as a function of Li-AHA concentration in aqueous medium, viz., the variation of pH, average 'aggregates' size from DLS measurements, UV-vis absorbance and the zeta potential corresponding to various dispersions. In fact, the colloidal stability of MWNTs dispersion could

be explained on the basis of the variation of the zeta potential value and pH value of the corresponding MWNTs dispersion as a function of increased Li-AHA concentration.

Zeta potential (ζ-potential) defines the surface charge accumulated on the surface of CNTs in the aqueous medium that determines the stability of the CNTs dispersion. The particles with ζ-potential less than -30 mV and more than +30 mV are considered to be in the stable region [50]. N-MWNTs show the ζ-potential value of -29.2 mV, while that of D-MWNTs exhibit -19.3 mV, which suggests that the dispersion of unmodified MWNTs is in the unstable region. However, the addition of Li-AHA decreases the value of ζ-potential, which attains the stable range of ζ-potential value. ζ-potential value represents the type and amount of surface charge that originates due to the ionic groups present on the surface of the CNTs. It can be explained on the basis that with the addition of Li-AHA, the negatively charged species would be increased within the aqueous medium, which consequently increase the absolute ζ-potential value of Li-AHA modified MWNTs.

This observation has been further substantiated by the observed pH values of the corresponding dispersion, which suggest that with increase in Li-AHA content, pH value shifts towards the basic region. The variation of 'agglomerates' size of different nanotubes obtained from DLS measurement with varying concentration of Li-AHA is shown in Table 2. It is observed that the 'aggregates' size of the MWNTs decreases with increase in Li-AHA concentration. A similar result has been reported earlier, which also substantiates this observation [51]. However, the 'aggregates' size mentioned in the previous work shows higher variation of average size owing to the settling tendency of MWNTs 'aggregates' in the aqueous medium.

Table 2: Variation of several parameters as a function of Li-AHA concentration for the

two different types of MWNTs

N-MWNTs:Li-AHA (wt/wt)	1:1 (wt/wt)	1:4 (wt/wt)	1:6 (wt/wt)	1:8 (wt/wt)
pH	6.2	6.6	7.5	8.4
Zeta potential	-50.8	-56.4	-59.4	-63.4
Aggregate size from DLS (nm)	355.9	228.5	203.8	168.8
UV-vis absorbance value at 273nm	0.76	0.85	0.82	0.88
I_D/I_G	0.92	0.55	0.48	0.46
Specific surface value obtained from BET(m^2/gm)	102.3	98.7	78.3	42.5
D-MWNTs:Li-AHA (wt/wt)	1:1 (wt/wt)	1:4 (wt/wt)	1:6 (wt/wt)	1:8 (wt/wt)
pH	7.4	7.9	8.7	9.3
Zeta potential	-28.5	-30.5	-31.6	-31.8
Aggregate size from DLS (nm)	400.2	239.9	204.4	182.5
UV-vis absorbance value at 273nm	0.63	0.73	0.84	0.86
I_D/I_G	1.05	0.68	0.51	0.49
Specific surface value obtained from BET(m^2/gm)	52.7	34.5	12.6	8.5

A similar magnitude of 'aggregates' size for modified MWNTs has been reported earlier [52]. In

this work, the variation in the 'average' size is quite moderate as the suspended particles are only

considered in this experiment. A decrease in 'aggregates' size of Li-AHA modified MWNTs is

observed, which suggests Li-AHA is able to dis-entangle the nanotubes 'agglomerates' into

several smaller 'agglomerates'. The adsorption of modifier molecule also depends on the type of

surfactant used [53]. It was reported that the 'aggregates' size of the MWNTs decreases in the

presence of surfactant however, the extent of decrease was varied depending on the surface area

and functionality of the surfactant used. Table 2 also shows the variation of UV-vis absorbance

at 273 nm as a function of Li-AHA concentration in Li-AHA modified MWNTs. The absorbance value increases with increase in Li-AHA content in the aqueous medium and the trend of variation of absorbance values remains same irrespective of the type of MWNTs. In general, the individual nanotubes absorb at ~ 273 nm in the UV-visible range and the corresponding UV-vis absorbance value represents the concentration of 'individualized' MWNTs present in the dispersion [27]. Hence, the increase in UV-vis absorbance value indicates 'de-agglomeration' of MWNTs (presence of higher concentration of 'individualized' MWNTs) [54-55]. The dispersion state of MWNTs is influenced by the concentration of surfactant (SDS) [19]. It has been reported that the UV-Vis absorbance value is increased up to certain concentration of surfactant, but afterwards leads to 're-aggregation' of MWNTs due to micelle formation. In the present context, 're-aggregation' could not occur due to the structural difference between Li-AHA and the classical surfactant, wherein Li-AHA consists of hydrophobic middle segment and hydrophilic ends. With the increase in Li-AHA content, it forms an adsorbed layer on the surface of MWNTs (confirmed through the increase in average diameter of MWNTs). This may eventually decrease the specific surface area corresponding to Li-AHA modified MWNTs as observed from BET analysis.

The variation in ordered graphitic structure of the MWNTs in the presence of Li-AHA has been studied through Raman spectroscopic analysis using the parameter I_D/I_G ratio provided in the Table 2. It has been reported that the decrease in the value of I_D/I_G ratio indicates an increase in the intensity of the tangential mode due to the 'de-agglomeration' of SWNTs [56]. In the present context, the value of the I_D/I_G ratio for Li-AHA modified MWNTs decreases with increase in Li-AHA content. The addition of Li-AHA leads to MWNTs 'agglomerates' of smaller size. Moreover, in the presence of Li-AHA, dis-entanglement of MWNTs 'agglomerates'

leads to the exposure of more graphitic (ordered) structure of MWNTs, which otherwise may

increase the intensity of the G-band [38]. However, at all ratios of MWNTs:Li-AHA mixture, the

value of I_D/I_G for Li-AHA modified D-MWNTs is observed to be higher as compared to Li-AHA
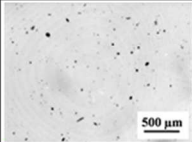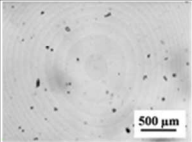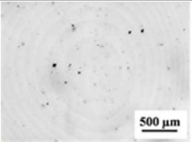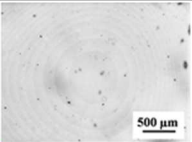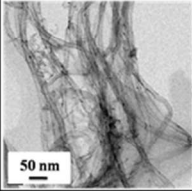
modified N-MWNTs.
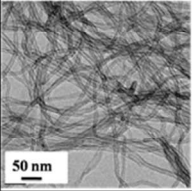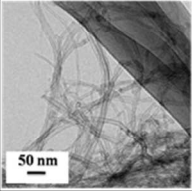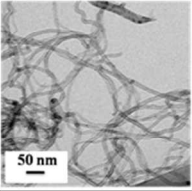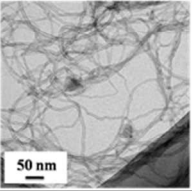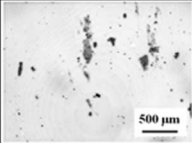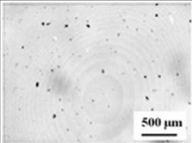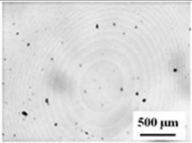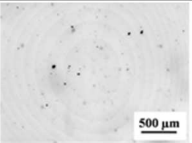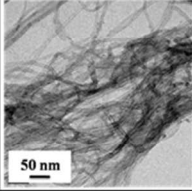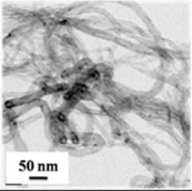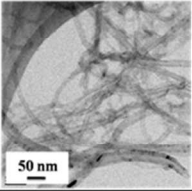
N-MWNTs:Li-AHA (wt/wt)	1:1 (wt/wt)	1:4 (wt/wt)	1:6 (wt/wt)	1:8 (wt/wt)
Optical micrographs				
Average 'Agglomerates' size (μm)	58.4	43.5	22.6	18.6
TEM micrographs				
Average Diameter (nm)	11.6	12.1	13.6	14.6
D-MWNTs:Li-AHA (wt/wt)	1:1 (wt/wt)	1:4 (wt/wt)	1:6 (wt/wt)	1:8 (wt/wt)
Optical micrographs				
Average 'Agglomerate' size (μm)	123.5	86.3	53.1	30.4
TEM micrographs				
Average Diameter (nm)	14.1	14.8	15.2	15.8

Figure 6: Average diameter and average 'agglomerates' size for both N-MWNTs and D-

MWNTs as a function of Li-AHA concentration from TEM and optical microscopic analysis

respectively

This result may be explained on the basis that low content of Li-AHA was not sufficient enough to 'de-agglomerate' the highly entangled 'agglomerates' of D-MWNTs of higher 'agglomerates' strength, which leads to comparatively higher 'agglomerates' structure along with 'individualized' MWNTs as compared to N-MWNTs. However, at higher concentration of the modifier, the I_D/I_G ratio for both N-MWNTs and D-MWNTs attains a similar value, which dictates that at higher concentration of the modifier, the content of ordered graphitic structure for both the MWNTs is in the same range. The modification of MWNTs with Li-AHA has shown an upshift in G-band to 1582 cm^{-1} for 1:6 N-MWNTs:Li-AHA and to 1580 cm^{-1} for 1:6 D-MWNTs modified with Li-AHA. A similar observation has also reported by Sreekanth et al. [27] for Li-AHA modified MWNTs and for Na-AHA modified MWNTs [57]. The upshift in G-band indicates strong interaction between MWNTs and Li-AHA. A similar observation has also been reported by earlier studies [27, 25]. It has been discussed that addition of Li-AHA to MWNTs 'agglomerates' leads to the adsorption of modifier layer onto the surface of MWNTs and the thickness of the layer is also increased with increase in the modifier content, which will be substantiated by TEM micrographs in the later section.

XPS is an analytical tool that provides the compositional analysis of the pristine and as well Li-AHA modified MWNTs. It provides elemental composition and depicts the functionalities associated with the respective element. This information can be obtained by de-convoluting the peaks corresponding to the elements. It is observed (Figure 7, Figure 8) that N-MWNTs contain 1.5 atomic% of oxygen and 98.5 atomic% of carbon. A similar observation has also reported by Datsyuk et al. [58]. It has been reported that MWNTs have shown sharp peak at 284.1 eV, which corresponds to the C1s graphitic peak [59].
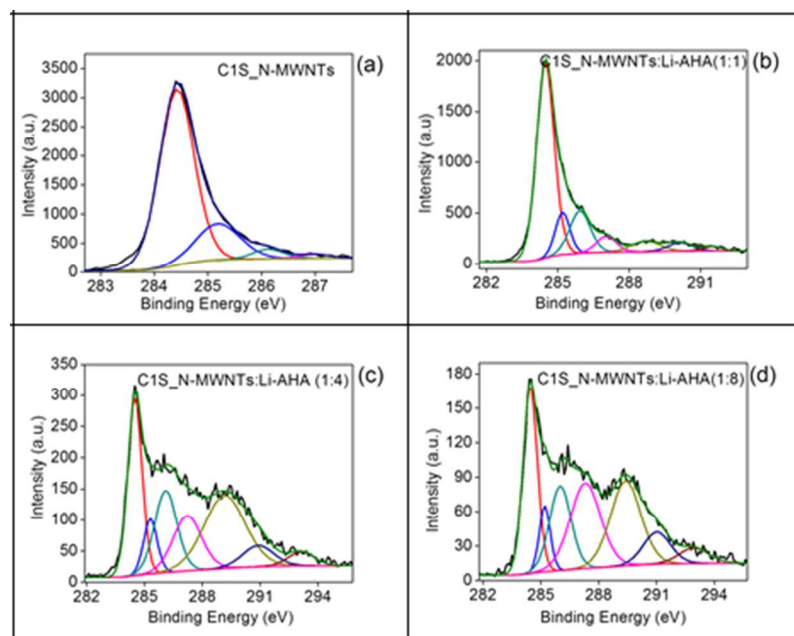
Figure 7: XPS plots for C1s peak for (a) N-MWNTs (b) N-MWNTs: Li-AHA (1:1)(wt/wt) (c) N-MWNTs:Li-AHA (1:4)(wt/wt) and (d) N-MWNTs:Li-AHA (1:8)(wt/wt)

Further, it is observed (Figure 7 and Figure 8) that nitrogen content increases linearly and the graphitic carbon content decreases with increase in the Li-AHA concentration. Addition of Li-AHA to MWNTs, leads to the adsorption of amine group on the MWNTs surface. De-convolution of C1s peak of N-MWNTs suggests that three peaks at 284.42, 285.12, 286.12 e.V correspond to sp^2 graphitic carbon; -C-OH and –C=O respectively. All the compositions show the peak at 290 and 292 e.V, which corresponds to the π-π* shake up feature that make the analysis more difficult. Even de-convolution of O1s peak also suggests the presence of -C-O bond in N-MWNTs and the atomic percentage also increases with increase in the modifier content.
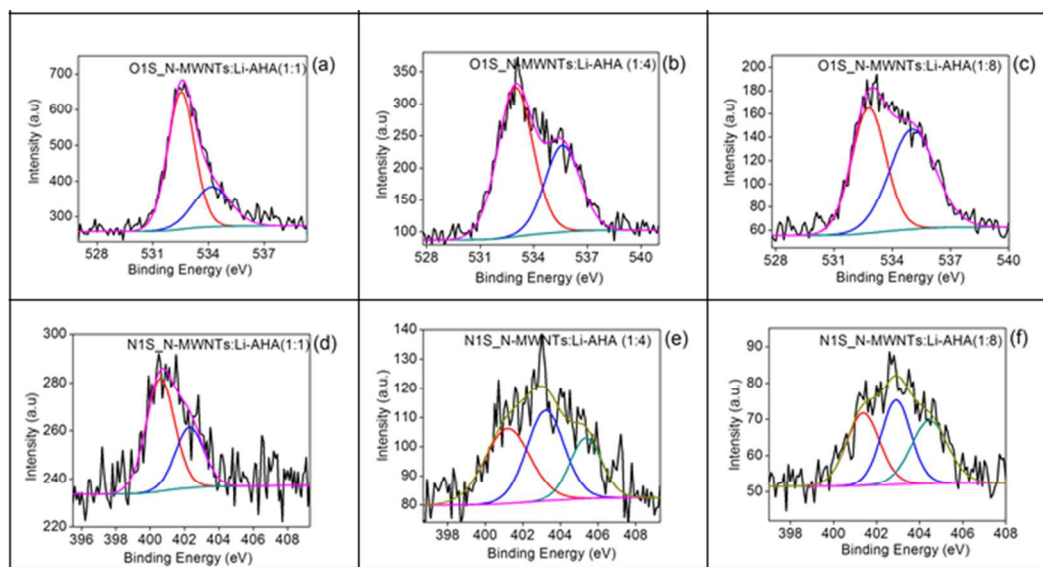
Figure 8: XPS plots for O1s and N1s peak for (a,d) N-MWNTs: Li-AHA (1:1)(wt/wt) (b, e) N-MWNTs:Li-AHA (1:4)(wt/wt) and (c,f) N-MWNTs:Li-AHA (1:8)(wt/wt) respectively

Wang et al. [60] has reported the thermodynamic and kinetic stability of the surfactant induced dispersion. The individually isolated state of the nanotubes has been considered to be the most thermodynamically stable state. In case of nanotubes-surfactant system, due to the adsorbed layer on the surface of the CNTs, the steric hindrance may also be responsible for the electrostatic repulsion between the CNTs. However, for surfactant, there exists a critical micelle concentration above which 're-aggregation' of the surfactant takes place [19], which may be substantiated via the decrease in the UV-vis absorbance value of MWNTs after a critical concentration of surfactant. However, in this work, it has been observed that the value of UV-vis absorbance increases with increase in Li-AHA content. Hence, Li-AHA can be considered as a more efficient modifier to enhance the 'de-agglomeration' of MWNTs 'agglomerates'. The 'de-agglomeration' of MWNTs 'agglomerates' is primarily governed by the following two factors – electrostatic force of repulsion [61] between the negatively charged MWNTs and AHA⁻, along with the steric hindrance [62] associated with the presence of five -CH$_2$ group present in the

organic modifier, Li-AHA. Several researchers [25-27] have proposed the plausible mechanism of 'de-agglomeration' of MWNTs 'agglomerates' in the presence of Li-AHA. It may be postulated that ultra-sonication leads to cavitation and creates spaces in the MWNTs bundles, which further allows the penetration as well as adsorption of Li-AHA on the surface of MWNTs. This leads to the dis-entanglement of MWNTs 'agglomerates' due to strong electrostatic repulsion between the negatively charged MWNTs and AHA^- species of Li-AHA, thus overcoming inter-tube van der Walls force of attraction. Moreover, the existence of modifier layer on the MWNTs surface due to hydrophobic interaction can be witnessed via TEM micrographs (Figure 6). The proposed mechanism may further be substantiated by the variation in zeta potential value with increase in Li-AHA content, which exceeds the barrier energy for coagulation process. It has been mentioned earlier that the non-covalent modifier dissociates into Li^+ and AHA^- ions. [40] The Li^+ ion would have a significant role in producing electrical double layer around the MWNTs 'agglomerates' that further help in exceeding the barrier energy for coagulation. This process may eventually help in improving the stability of MWNTs dispersion in the aqueous medium.

d. Effect of Li-AHA on the electrical conductivity of Li-AHA modified MWNTs pellets

MWNTs are mainly considered as a coaxial tubular form of graphene sheet forming several walls around the thin sheet of graphene layer. In general, there exists an interlayer spacing of ~0.34 nm [63] between the walls of the individual nanotubes, which closely resembles the interlayer distance between graphite the sheet, which is ~0.335 nm. The intrinsic electrical conductivity of MWNTs depends on several factors; viz., diameter, number of walls and the defects present in a given MWNTs. It also depends on the process of synthesis of nanotubes as it has been observed that MWNTs obtained from arc-discharge method possess diameter of ~20

nm, while diameters ranging even upto 100 nm for MWNTs obtained from CVD technique [64]. In the present context, DC electrical conductivity of the pristine and Li-AHA modified MWNTs samples have been measured on compacted MWNTs pellets. Pristine D-MWNTs exhibit lower DC electrical conductivity value as compared to unmodified N-MWNTs. This result is in conformity with the result obtained from Raman spectroscopic analysis, which shows that the I_D/I_G value is higher for D-MWNTs as compared to N-MWNTs. It has been studied earlier that the electrical conductivity of MWNTs varies inversely with the diameter of the tubes. Hence, the number of walls possessed by the CNTs also affects the ballistic electrical conduction of MWNTs. Further, D-MWNTs exhibit lower purity as compared to N-MWNTs, which also contributes to the variation in electrical conductivity of D-MWNTs with respect to N-MWNTs. It has been studied [53] that as arc-discharge produced MWNTs are grown at higher temperature, thus produces clearer MWNTs as compared to MWNTs produced from CVD technique. However, this work is restricted to the electrical conductivity of two types of MWNTs produced by CVD technique.
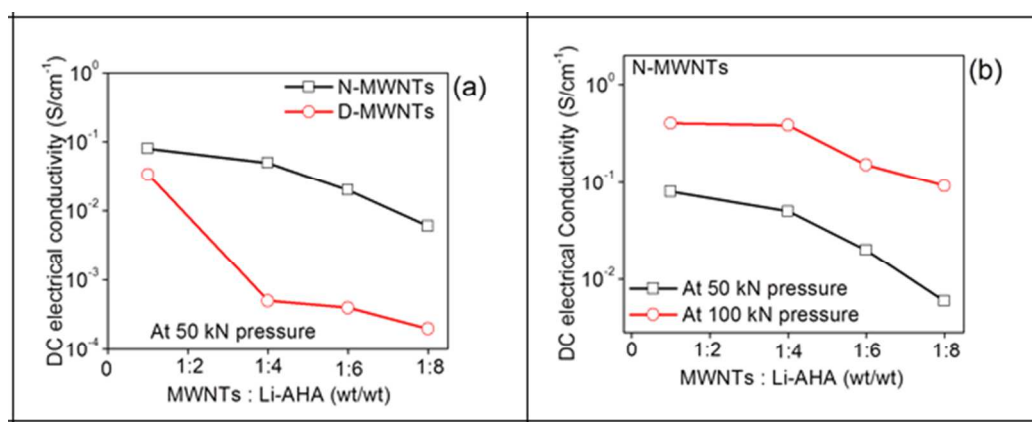

Figure 9: Variation of DC electrical conductivity of MWNTs as a function of modifier concentration in Li-AHA modified MWNTs pellets

Figure 9a shows the electrical conductivity of N-MWNTs pellets decreases with increase in modifier content obtained at 50 kN pressure level. A same trend is observed for the electrical conductivity values for Li-AHA modified N-MWNTs pellets at different pressure level of 50 kN and 100 kN (Figure 9b). It is known that the transport of electrons along the nanotubes takes place through the outer walls of MWNTs and the continuous transport of electrons facilitates through the increase in the number of contact points between the CNTs 'agglomerates'. Owing to the surface coverage of N-MWNTs with Li-AHA, the contact between the MWNTs 'agglomerates' may get restricted, which results in a decrease in DC electrical conductivity value of the Li-AHA modified N-MWNTs. Thus, the surface modification of MWNTs with Li-AHA leads to the formation of layers of modifier on the surface of MWNTs, which eventually decreases the electrical conductivity of the Li-AHA modified MWNTs pellets.

The increase in diameter of the MWNTs is due to the adsorption of the organic modifiers on the MWNTs surface. Similar results have been reported by Xin [65], where increase in the diameter of CNTs has been observed with increase in modifier concentration. The multilayer formation of modifier on the CNTs surface leads to the separation of CNTs 'agglomerates' and as a result of this, specifically at higher concentration of modifier, the thickness of the modifier layer on CNTs surface becomes so high that the inter-spacing between two adjacent CNTs is increased. The increase in inter-spacing between two CNTs may hinder the continuous network structure of the CNTs and thus, may lead to a decrease in the electrical conductivity. However, at comparatively lower concentration of the modifier, the layer thickness is moderately lower, thus facilitates the formation of conductive pathway for tunneling. Moreover, at lower concentration of Li-AHA, the electrical conductivity of modified CNTs seems to be higher. The existence of Li-AHA layer on the MWNTs surface can be further confirmed from the TEM micrographs

(figure 10). The micrographs further exhibit that with increase in modifier content, the thickness

of the modifier layer also increases. The thickness of the modifier layer ranges from 0.4 nm (for

N-MWNTs:Li-AHA of 1:1) to 0.9 nm (for N-MWNTs:Li-AHA of 1:8). Till date, there exists a

controversy that how the organic carbon layers could be adsorbed on the surface of the CNTs. In

this work, an attempt has been made to explain the above observations. From literatures, it can

be obtained that [66] the atomic diameter of carbon is ~ 0.154 nm. Hence, it can be observed that

as the modifier content is increased, the number of Li-AHA molecule adsorbed onto the CNTs

would also increase. It can be estimated that at the modification ratio of 1:1 (wt/wt), there may

exist approximately 4 layers corresponding to 0.4 nm and the number of layer may be increased

to 9 as the modifier ratio increased to 1:6 of MWNTs:Li-AHA. The adsorbed layer creates

defects or served as an insulating organic layer of modifier on CNTs surface that disrupts the

continuous flow of electrons along the MWNTs network. Moreover, a relationship could be

observed between the DC electrical conductivity of the MWNTs and that of the pressure applied

on the MWNTs to form their pellets. With increase in the magnitude of pressing pressure during

compaction, the DC electrical conductivity value also increases. This can be explained on the

basis that with increase in the applied pressure, the connectivity between the MWNTs

'agglomerates' could be enhanced and Li-AHA may leach out from the modified MWNTs

'agglomerates' and accelerates the transportation of electrons between the MWNTs
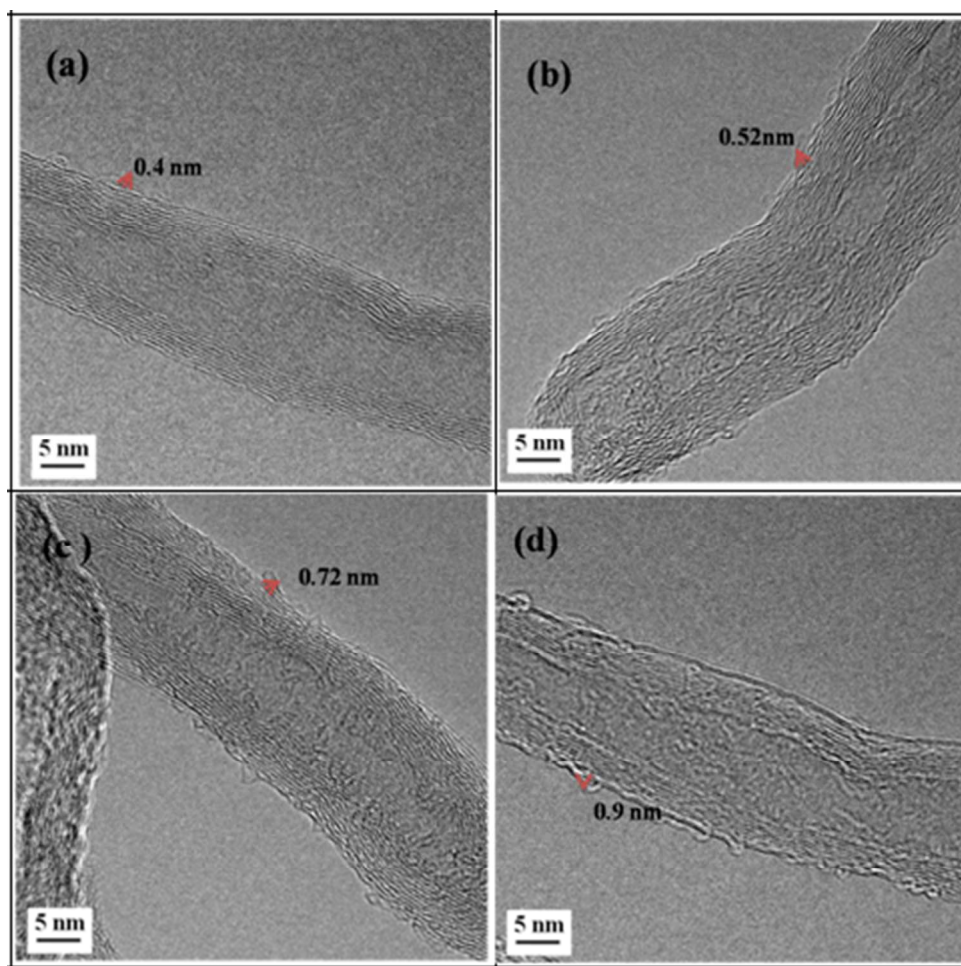
'agglomerates'.

Figure 10: TEM micrographs of N-MWNTs: Li-AHA mixture of (a)1:1 (b)1:4 (c)1:6 and (d)
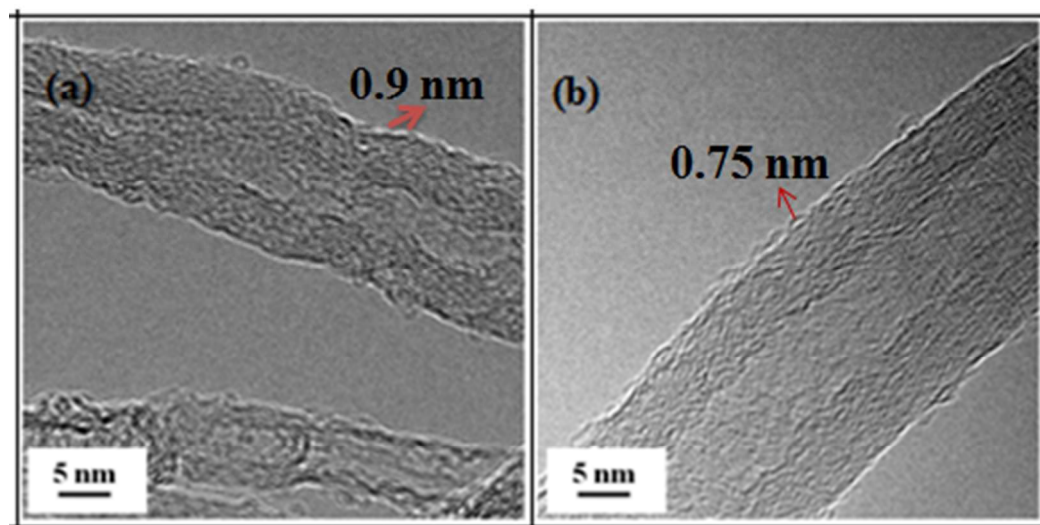
1:8 (wt/wt)

Figure 11: TEM micrographs of (a) N-MWNTs:Li-AHA (1:8)(wt/wt) (b) D-MWNTs:Li-AHA

(1:8)(wt/wt) mixture

Conclusion

'Agglomeration' behaviour of the MWNTs has been investigated for two types of MWNTs of varying 'agglomerates' size and varying extent of entanglements. The current investigation has shown higher extent of entanglements and higher average 'agglomerates' size corresponding to D-MWNTs as compared to N-MWNTs. In order to overcome 'agglomerated' structure associated with MWNTs, a novel organic modifier (Li-AHA) has been utilized.

Nano-indentation experiment has been carried out for the compacted MWNTs pellets, which has indicated higher 'agglomerates' strength associated with D-MWNTs as compared to N-MWNTs. It has been also observed that Li-AHA has led to a porous 'agglomerated' structure in Li-AHA modified MWNTs as suggested via BET analysis and nano-indentation experiment. Normalized Young's modulus of MWNTs was increased progressively as a function of Li-AHA

concentration in the compacted Li-AHA modified MWNTs pellets, which indicated a higher Young's modulus corresponding to 'individualized' MWNTs as compared to 'agglomerated' MWNTs.

Further, FACS experiment has been shown to be an efficient technique to assess the extent of dispersion of MWNTs 'agglomerates' in the aqueous medium. FACS analysis has indicated a decrease in FSC value (denotes a decrease in 'agglomerates' size) with the increase in SSC value (denotes increase in granularity) for MWNTs/Li-AHA mixture with increased concentration of Li-AHA in the de-ionized water.

Average 'agglomerates' size corresponding to Li-AHA modified MWNTs has decreased with increase in Li-AHA concentration, which has indicated the breakdown of bigger 'agglomerates' into smaller 'agglomerates' as well as 'individualized' MWNTs in the presence of Li-AHA. The zeta potential value has indicated that Li-AHA has led to a further decrease in the zeta potential value of stable range of colloidal dispersion. The presence of 'individualized' MWNTs could also be observed in the presence of Li-AHA via UV-vis spectroscopic analysis.

Further, electrostatic repulsion has been identified as the driving force for 'de-agglomeration' of MWNTs in the de-ionized water, wherein, Li-AHA dissociates in to Li^+ and AHA^-. During ultra-sonication, a higher extent of negatively charged AHA^- species could enter in the MWNTs 'agglomerates' and could develop electrical double layer around MWNTs 'agglomerates'. This phenomenon could eventually lead to 'individualized' MWNTs along with smaller 'agglomerates'.

In brief, it may be concluded that the role of Li-AHA in breakdown of MWNTs 'agglomerates' has been thoroughly understood from the various experiments performed with

bulk MWNTs as well as aqueous dispersion of MWNTs. Li-AHA has been shown to very effective to 'de-agglomerate' MWNTs in the de-ionized water.

Acknowledgement

References

1. J. Koohsorkhi, Y. Abdi, S. Mohajerzadeh, H. Hosseinzadegen, Y. Komijani and E. A. Soleimani, *Carbon*, 2006, **44**, 2797-2803.

2. X. Tang , S. Bansaruntip, N. Nakayama, Y. L. Erhan, Y. L. Chang and Q. Wang, *Nano lett.*, 2006, **6**, 1632-1636.

3. C. A. Mitchell and R. Krishnamoorti, *Macromolecules,* 2007, **40**, 1538 -1545.

4. R. H. Baughman, A. A. Zakhidov and W. A. De Heer, *Science,* 2002, **297**, 787-792.

5. M. Rahmat and P. Hubert, *Compos. Sci. Technol*., 2011, **72**, 72-84.

6. O. Breuer and U. Sundararaj, *Polym. Compos*., 2004, **25**, 630 – 645.

7. M. T. Müller, B. Krause, B. Kretzschmar and P. Pötschke, *Compos. Sci Technol.*, 2011,**71**,1535- 1542.

8. Y. Zeng, P. Liu, J. Du, L. Zhao, P. M. Ajayan and H. M. Cheng, *Carbon,* 2010, **48**, 3551-3558.

9. M. Morcom, K. Atkinson and G. P. Simon, *Polymer,* 2010, **51**, 3540-3550.

10. R. Socher, B. Krause, M. T. Müller, R. Boldt, P. Pötschke, *Polymer,* 2012, **53**, 495–504

11. F. Y. Castillo, R. Socher, B. Krause, R. Headrick, B. P. Grady, R. Prada-Silvy, P. Pötschke, *Polymer,* 2011, **52**, 3835–3845

12. S. Sathyanarayana, C. Hübner, J. Diemert, P. Pötschke, F. Henning, *Compos. Sci. Technol.*, 2013, **84**, 78–85

13. J. M. Benard, T. Stora and W. Heer, *Adv. Mater.,* 1997, **9**, 827-830.

14. B. Vigolo, A. Penicaud, C. Coulon, C. Sauder, R. Pailler and C. Journet, *Science*, 2000, **290**, 1331-1334.

15. K. Esumi, M. Ishigami, A. Nakajima, K. Sawada and H. Honda, *Carbon,* 1996, **34**, 279-281.

16. D. H. Jung, Y. K. Ko and H. T. Jung, *Mat. Sc. and Eng.*, 2004, **24**, 117-121.

17. Y. Kim, S. M. Kwon, D. Y. Kim, H. S. Kim, H. J. Jin, *Current Appl. Phys.*, 2009, **9**, 100-103.

18. L. Vaisman, H. D. Wagner and G. Marom, *Adv. In Colloid and Inter. Sci.*, 2006, **128**-136, 37-46.

19. L. Jiang, L. Gao and J. Sun, *J. Colloid Inter. Sci.,* 2003, **260**, 89-94.

20. B. Pan and B. Xing, *Environ. Sci. Technol*., 2008, **42**, 9006-9013.

21. L. Ju, W. Zheng, X. Wang, J. Hu, Y. Zhang, *Colloids and surf. A: Physicochem. Eng. Aspects*, 2012, **409**, 159-166.

22. B. Vigolo, C. Coulon, M. Maugey, C. Zakri and P. Poulin, *Science*, 2005, **303** (5736), 920-923.

23. R. Rastogi, R. Kaushal, S. K. Tripathi, A. L. Sharma, I. Kaur and L. M. Bharadwaj, *J. Colloid Int. Sci.,* 2008*, **328**, 421-428.

24. Q. Chen, C. Saltiel, S. Manickavasagam, L. Schadler, R. W. Siegel and H. Yang, *J. Colloid Int. Sci.,* 2004, **280**, 91-97.

25. J. Rausch, R. C. Zhuang and E. Made, *Compos. :Part A*, 2010, **41**, 1038-1046.

26. N. Mukhopadhyay, A. R. Bhattacharyya, A. S. Panwar, I. Samajdar and G. Kumar , *Phys. Chem. Chem. Phys.*, 2015, **17**, 4293- 4310.

27. M. S. Sreekanth, A. S. Panwar, P. Pötschke and A R. Bhattacharyya, *Phys. Chem. Chem. Phys.*, 2015, **17**, 9410-9419.

28. K. Kendall and T. P. Weihs, *Appl. Phys. (Berl.),* 1992, **25**, A3-A8.

29. Y. Raichman, M. Kazakevich, E. Rabkin and Y. Tsur, *Adv. Mater.,* 2006, **18**, 2028–2030.

30. D. Cai, D. Blair, F. J. Dufort, M. R. Gumina, Z. Huang, G. Hon, D.Wagner, D. Canhan, K. Kempa, Z. F. Ren and T. C. Chiles, *Nanotechnology*, 2008, **19**, 345102, 1-10.

31. H. Haniu, N. Saito, Y. Matsuda,Y. A. Kim, K. C. Park, H. Kato, K. Nakamura, K. Hara, K. Aoki, K. Takanashi and Y. Usui, *Inter. J. of Nanomed.*, 2011, **6**, 3295–3307.

32. N. A. Sakharova, J. V. Fernandes, J. M. Antunes**, *Int. J. of Sol. and Str.,* 2009, **46** (5), 1095-1104.

33. A. V. Poyekar, A. R. Bhattacharyya, A. S. Panwar and G. P. Simon, *Polym. Eng. Sci.*, 2015, **55** (2), 429-442.

34. H. Farhat , K. Sasaki , M. Kalbac , R. Saito , M. S. Dresselhaus , M. Hoffmann and J. Kong , *Phys. Rev. Lett.,*2009, **27**, 102 (2), 126804, 1-4.

35. R. A. DiLeo , B. J. Landi and R. P. Raffaelle , *J Appl Phys.*, 2007,**101**(6), 64301-15.

36. A. Gupta, P. Joshi, G. Chen, S. Tadigadapa and P. C. Eklund, *Nano Lett.,* 2006, **6**, 12, 2667 – 2673.

37. M. J. Tomas, *Chem Eng Sci.,* 2007*,* **62** (7), 1997–2010.

38. I. Alig, G. R. Kasaliwal, P. Pötschke and D. Lellinger, *Polymer,* 2012, 53, 4-28.

39. L. A. Girifalco, M. Hodak and R. S. Lee, *Phys. Rev. B,* 2000, **62**, 13104 - 13110.

40. S. Bose, A. R. Bhattacharyya, R. A. Khare, A. R. Kulkarni, P. Sivaraman and T. U.Patro, *Nanotechnology*, 2008, **19**, 335704 – 1-8.

41. J. Hilding, E. A. Grulke, Z. G. Zhang , *J Disper. Sci. Technol.*, 2003, **24**, 1–41.

42. C. Schild and A. Kwade, *J. Mater. Res*., 2012, **27**, 672- 684.

43. B. Bhusan, Handbook of Nanotechnology, Springer Heidelberg Dordrecht London, New York, 3rd edition, 2010.

44. W. C. Oliver and P. M. Pharr, *J Mater. Res.,* 1992, **7**, 1564-1583.

45. W. C. Oliver and G. M. Pharr, *J Mater. Res.,* 2004, **19**, 3-20.

46. J. Gong, Z. Peng and H. Miao, *J. of Euro. Ceram. Soc.,* 2005, **25**, 649-654

47. R. P. Haughland, The Handbook: A Guide to Fluorescent Probes and Labeling Technologies, 10th edition, Molecular Probes, 2005.

48. M. D. Tiwari, G. H. Sagar, and J. R. Bellare, *Langmuir,* 2012, **28**, 4939-4947.

49. A. V. Poyekar, A. R. Bhattacharyya, A. S. Panwar, G. P. Simon, and D. S. Sutar, *ACS Appl. Mater. Interf.*, 2014, **6**, 11054−11067.

50. B. White, S. Banerjee, S. O'Brien, N. J. Turro and I. P. Herman , *J. Phys. Chem. C*, 2007, **111**, 13684-13690.

51. R. A. Khare, A. R. Bhattacharyya, A. S. Panwar, S. Bose and A.R. Kulkarni, *Polym. Eng. Sci.,* 2011, **51**, 1891-1905.

52. W. H. Chang, I W Cheong, S. E. Shim and S. Choe, *Macromol. Res.*, 2006, **14**, 545-551.

53. L. Vaisman , G. Marom and H. D. Wagner, *Adv. Funct. Mater.,* 2006, **16**, 357-363.

54. K. Saitn-Aubin, P. Poulin, H. Saadaoui, M. Maugey, and C. Zakri, *Langmuir, 2009,* **25** *,* 13206–13211.

55. J. Yu, N. Grossiord, C. R. Koning and J. Loos, *Carbon*, 2007, **45**, 618-623.

56. S. S. Strano, V. C. Moore, M. K. Miller, M. J. Allen, E. H. Haroz, C. Kittrell, R. H. Hauge and R. E.Smalley, *J. Nanosci. Nanotechnol.,* 2003, **3**, 81−86.

57. P. V. Kodgire, A. R. Bhattacharyya, S. Bose, N. Gupta, A. R. Kulkarni and A. Misra , *Chem. Phys. Lett.,* 2006, **432**, 480–485.

58. V. Datsyuk, M. Kalyva, K. Papagelis, J. Parthenios, D.Tasisb, A. Siokou, I. Kallitsis and C. Galiotis, *Carbon*, 2008, **46**, 833 − 840.

59. H. Ago, T. Kugler, F. Cacialli, W. Salaneck, M. Shaffer, A. Windle, R. Friend, *J. Phys. Chem. B,* 1999,**103**,8116–8121.

60. H. Wang, Curr. Opinion *Colloid Int. Sci*., 2009, **14**, 364-371.

61. M. J. O'Connell, S. M. Bachilo, C .B. Huffman, V. C. Moore, M. S. Strano, E. H. Haroz, K. L. Rialon, P. J. Boul, W. H. Noon, C. Kittrell, J. P. Ma, R. H. Hauge, R. B. Weisman, and R. E. Smalley, *Science*, 2002, **297**, 593-596.

62. R. Bandopadhyay, E. Nativ-Roth, O. Regev, and R. Yerushalmi-Rozen, *Nano Lett.,* 2002, **2**, 25-28.

63. P. M. Ajayan, *Chem. Rev.,* 1999*,* **99**, 1787-1800.

64. P. R. Bandaru, *J. Nanosci. Nanotechnol*., 2007, **7**, 1–29.

65. D. Lin and B. Xing, *Environ. Sci. Technol*., 2008, **42,** 5917-5923.

66. J. Emsley, The *Elements*, 3rd edition., Oxford, Clarendon Press, 1998.

Graphical Abstract

Ultra-sonication induced opening/gap in the 'agglomerates' of the MWNTs, which on modification with Li-AHA leads to break-down of MWNTs 'agglomerates' via electrostatic charge repulsion between the negatively charged species. On solidification, Li-AHA adsorbs on the MWNTs surface.